

On the completeness of contraction map proof method for holographic entropy inequalities

Ning Bao^{a,b} Keiichiro Furuya^a Joydeep Naskar^{a,c}

^a*Department of Physics, Northeastern University, Boston, MA, 02115, USA*

^b*Computational Science Initiative, Brookhaven National Laboratory, Upton, NY 11973 USA*

^c*The NSF AI Institute for Artificial Intelligence and Fundamental Interactions, Cambridge, MA, U.S.A.*

E-mail: ningbao75@gmail.com, k.furuya@northeastern.edu,
naskar.j@northeastern.edu

ABSTRACT: The contraction map proof method is the commonly used method to prove holographic entropy inequalities. Existence of a contraction map corresponding to a holographic entropy inequality is a sufficient condition for its validity. But is it also necessary? In this note, we answer that question in affirmative for all linear holographic entropy inequalities with rational coefficients. We show that, generically, the pre-image of a non-contraction map is not a hypercube, but a proper cubical subgraph, and show that this manifests as alterations to the geodesic structure in the bulk, which leads to the violation of inequalities by holographic geometries obeying the RT formula.

Contents

1	Introduction	1
2	Review of the Contraction Map Proof Method	4
2.1	Contraction map	4
2.2	Graphs and holographic geometries of HEI from bitstrings	5
3	Lessons from Simple Scenarios	8
3.1	Deforming the Monogamy of Mutual Information	9
3.2	A Five-Party Example	12
3.3	Non-contraction and Geometry	13
4	Main theorem	16
4.1	Mathematical proof	17
5	Discussion	21
5.1	Completeness of the algorithmic method to generate all the HEIs	21
5.2	Interpretations of the HEIs	22
5.3	Entanglement wedge nesting and geometry-graph duality	22

1 Introduction

Quantum entanglement is an ubiquitous phenomenon of nature appearing in many different contexts of quantum physics, and quantum gravity is no exception. The *AdS/CFT* correspondence [1] has proven to be a hugely successful tool to understand various aspects of quantum gravity, at least perturbatively. By virtue of this correspondence, the structure of quantum entanglement in a boundary CFT mysteriously encodes the information about the geometry of the dual bulk theory of gravity. A part of that mystery has been unfolded by the Ryu-Takayanagi (RT) formula[2], which relates the entanglement entropy of a subregion R of the boundary CFT to the minimal surface γ_R in the bulk homologous to R . More precisely,

$$S(R) = \frac{\text{area}(\gamma_R)}{4G_N}, \tag{1.1}$$

where G_N is the Newton's constant. This formula holds up to leading order in $1/G_N$, and for $O(G_N^0)$ corrections, one analogously defines the quantum extremal surface [3, 4]. However, for the purpose of this paper, we will strictly restrict ourselves to the leading order contribution, i.e., the validity of our statements hold upto $O(1/G_N)$.

It is, however, important to clarify that the validity of the RT formula assumes the existence of a semi-classical bulk dual, and not every quantum state on the boundary CFT

admits one. We will therefore only talk about those states that admit a semiclassical dual, and are known as *holographic states*. But can we say anything about which states are holographic? It is generally not known, to the best of our knowledge, what are the sufficient conditions for the existence of a bulk dual, however, we do know some necessary ones. A natural question to ask is that since boundary entanglement is so intricately related to the bulk geometry, what can we learn about the bulk geometry by studying entanglement entropy on the boundary CFT? The authors in [5] were the first to ask this question, which led to the formulation of the holographic entropy cone (HEC). A series of interesting works followed this development, see references [6–15] for a partial list¹.

The HEC is a rational, polyhedral, convex cone defined by its facets, that are given by a finite set of independent, linear inequalities involving subregion entropies. These inequalities, also known as *facet inequalities* bound the entropic phase space of holographic states. In other words, these inequalities are the independent set of tight holographic entropy inequalities (HEI) that cannot be improved further. The holographic entropy cone is completely known for up to five parties [5, 16], and partially known for six parties [17], and barring the exception of two infinite families[5, 18–20], largely unknown for higher parties.

The standard method to prove an HEI is the contraction map proof method (which we will review in section 2). It is proved in [5] that if a contraction map exists for a candidate conjecture inequality, then it is a valid HEI. But it remained an open question if the validity of an HEI implies the existence of a contraction map. In a previous work [21], we discovered several properties of the contraction map. These properties shed light on the rigidity of these maps as they admit several rules to deterministically fill up the entries of the contraction map, and at the same time incorporate the flexibility of these maps in terms of free choices. These properties strongly suggest that the entries of the contraction map is not just some constraint satisfaction tool, but are closely related to the space-like geodesic structure on the bulk slice. Contraction map can be thought of as an encapsulation of the inclusion/exclusion principle to encode bulk subregions. These ideas motivated us further investigate the contraction maps from the perspective of graph theory, which led to the discovery of the equivalence of contraction maps to graph contraction maps between hypercubes and partial cubes [15]. Exploiting this equivalence, we suggested an algorithmic procedure (albeit, a very slow one) to find all HEIs that have corresponding contraction maps².

All known facet HEIs discovered so far admit a contraction map, and there are no known HEI that does not have a contraction map. This is a strong evidence in favour of the completeness of the contraction map proof method. Moreover, the deterministic fixing of the entries of contraction maps and their geometric interpretation via inclusion/exclusion makes the case of completeness stronger, as false inequalities often demand bulk subregions to be included and excluded simultaneously, leading to the failure of contraction condition. Nevertheless, a formal proof of completeness has been elusive. In this work, we shed light

¹We apologize for providing partial list, that excludes many other interesting developments in this field.

²In a future work, we will report findings on some new HEIs discovered from partial cubes[22].

on this topic and give a proof of completeness, upto certain disclaimers. We will clarify them one by one,

- Our proof of completeness of contraction map proof method rely on the existence of a graph model corresponding to a smooth bulk geometry (and vice versa), which is achieved by a discrete partitioning of the bulk manifold by RT surfaces homologous to boundary subregions. In such models, the discrete entropy is computed on a graph by virtue of edge weights and a min-cut procedure ensures that it equals to the entanglement entropy of the boundary subregion corresponding to the cut. We expect that any sensible holographic geometry admits such a graph realization defined by entanglement entropies given by the RT formula and we are not aware of any counter-example.³
- Our work is closely derived following ideas of the holographic entropy cone. Therefore, the contraction map completion is proved for linear inequalities with rational coefficients realizable within the framework of HEC, applicable to both facet and non-facet HEIs. We do not rule out the possibility of non-linear inequalities.
- Our work borrows some of the lessons learned from the existing HEIs, their contraction maps and associated graph structures. We develop a mathematical machinery to define our physical insights. We take some of those insights, for instance, certain adjacency conditions, as physical requirements to construct our proof. We justify their existence and provide supporting evidence for the same.

Main Result and Organization

The main result of this paper is the following theorem:

Theorem 4.1. *Given a candidate entropy inequality,*

$$\sum_{i=1}^l \alpha_i S_{P_i} \geq \sum_{j=1}^r \beta_j S_{Q_j}, \quad \alpha_i, \beta_j \in \mathbb{Z}_+, \quad (1.2)$$

it is a valid HEI if and only if a contraction map $f : \{0, 1\}^M \rightarrow \{0, 1\}^N$ exists (where $M = \sum_i \alpha_i$ and $N = \sum_j \beta_j$) satisfying homology conditions on the boundary.

The idea of the proof goes as follows: we assume on the contrary that there exists a true HEI that does not have a contraction map. We show that it is possible to always find a geometry that violates the HEI. A non-contractive map breaks the adjacency between distances on graph and Hamming distance of bitstrings. Geometrically, this manifests as change in the geodesic structures in the bulk, thwarting the bulk smoothness. We show that such contradiction arises due to our incorrect assumption about the non-existence of a contraction map corresponding to the HEI. In fact, we will show that non-contraction

³On the other hand, we have examples of non-holographic theories, where the entanglement entropy follows an area law to obey HEIs [23, 24].

maps are always associated with alterations of the geodesic structure of the bulk manifold, such that always exists a holographic geometry for which the inequality is violated.

The organization of this paper is as follows. In section 2, we review the relation between geometry and graph, followed by the contraction map proof method. In section 3, we give examples of false inequalities and their failure to form contraction maps and go on discussing the implications of non-contraction maps on the bulk geometry. Moreover, we present an example of how a non-contraction map fails a valid HEI, such as MMI. In this section, we build the physical intuitions towards the proof of completeness. In section 4, we develop the mathematical machinery and write a formal proof of completeness. Lastly, we discuss the implications of our results and potential applications in section 5.

2 Review of the Contraction Map Proof Method

A n -party holographic entropy inequality (HEI) involving n disjoint regions (and a purifier O) $[n+1] := \{A_1, \dots, A_n, A_{n+1} = O\}$ can be written as

$$\sum_{i=1}^l \alpha_i S_{P_i} \geq \sum_{j=1}^r \beta_j S_{Q_j}, \quad (2.1)$$

where α_i and β_j for $i = 1, \dots, l$ and $j = 1, \dots, r$ are positive integers \mathbb{Z}_+ . P_i and Q_j are polychromatic subregions, which are the elements of the proper power set $P(\{A_1, \dots, A_n\}) \setminus \emptyset$ containing $2^n - 1$ possible elements. We can expand the inequality to have a unit coefficient for each term, i.e.,

$$\sum_{u=1}^M S_{L_u} \geq \sum_{v=1}^N S_{R_v}, \quad (2.2)$$

where $L_u, R_v \in P(\{A_1, \dots, A_n\}) \setminus \emptyset$ for $\forall u = 1, \dots, M$ and $\forall v = 1, \dots, N$, such that

$$\sum_{i=1}^l \alpha_i = M, \quad \sum_{j=1}^r \beta_j = N. \quad (2.3)$$

2.1 Contraction map

A contraction map is defined as follows.

Definition 2.1 (Contraction map). *A map $f : \{0, 1\}^M \rightarrow \{0, 1\}^N$ is a contraction map if, for $x, x' \in \{0, 1\}^M$,*

$$d_H(x, x') \geq d_H(f(x), f(x')). \quad (2.4)$$

Each side of the inequality is encoded to a set of bitstrings by *occurrence bitstrings*. The occurrence bitstrings of the LHS of the inequality are defined as, for each $A_k \in [n+1]$,

$$x_{A_k}^u = \begin{cases} 1, & A_k \in L_u \\ 0, & \text{otherwise} \end{cases} \quad (2.5)$$

where $x_{A_k}^u$ is the u -th bit of the bitstring $x_{A_k} \in \{0, 1\}^M$. Each bitstring $x \in \{0, 1\}^M$ represents a bulk subregion consisting a constant time slice of AdS_{D+1}/CFT_D partitioned

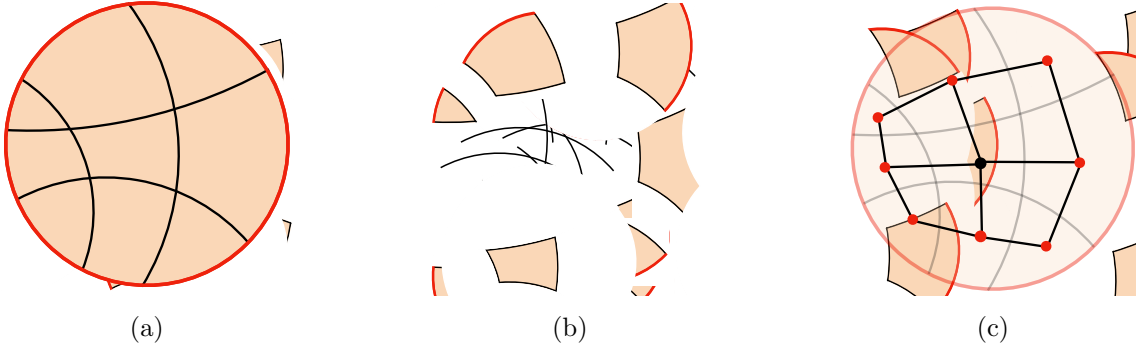


Figure 1: (a) A holographic geometry with the RT arrangement: Four RT surfaces denoted by black lines are arranged on a constant time slice of $\text{AdS}_3/\text{CFT}_2$. The boundary is colored red. (b) The RT arrangement partitions the time slice into bulk subregions. (c) The partial cube associated with the RT arrangement. The boundary vertices are shown in red. The vertex in the middle shown in black is a bulk vertex.

by a set of RT surfaces. The occurrence bitstrings $x_{A_k} \in \{0, 1\}^M$ and $y_{A_{k'}} \in \{0, 1\}^N$ for any $k, k' \in \{1, \dots, n+1\}$ represent the bulk subregions that are homologous to the boundary subregion A_k and $A_{k'}$. One requires a consistency of the homology conditions between the LHS bitstrings and those for the RHS bitstrings under a contraction map, i.e.,

$$f(x_{A_k}) = y_{A_k}, \quad \forall k \in \{1, \dots, n+1\}, \quad (2.6)$$

which imprints the inequality to the contraction map. Then, the contraction map satisfying the consistent homology conditions can be used to prove that the candidate entropy inequality is a valid HEI.

Theorem 2.1 (‘Proof by contraction’; HEI \leftarrow contraction map). [5] *Let $f : \{0, 1\}^M \rightarrow \{0, 1\}^N$ be a contraction map, i.e.,*

$$d_H(x, x') \geq d_H(f(x), f(x')), \quad \forall x, x' \in \{0, 1\}^M. \quad (2.7)$$

If $f(x_{A_k}) = y_{A_k}$ for $\forall k \in \{1, \dots, n+1\}$, then (2.2) is a valid n -party HEI.

For later purposes, we sketch the proof of theorem 2.1 in the next subsection after briefly reviewing the representations of holographic geometries with bitstrings and graphs.

2.2 Graphs and holographic geometries of HEI from bitstrings

For a given set of RT surfaces in a constant time slice of $\text{AdS}_{D+1}/\text{CFT}_D$, we have an RT arrangement⁴ that partitions the bulk manifold into a set of subregions in the bulk.

Definition 2.2 (RT arrangements in $\text{AdS}_{D+1}/\text{CFT}_D$). *Given a set of distinct boundary entanglement entropies in $\text{AdS}_{D+1}/\text{CFT}_D$ for some $D \in \mathbb{Z}_{\geq 2}$, $\{S_{L_u} | u \in [M]\}$, we have a set of distinct RT surfaces*

$$\Gamma_M = \{\gamma_{L_u} | u \in [M]\} \quad (2.8)$$

using the RT formula. Then, the arrangement of RT surfaces, or an RT arrangement, is the set Γ_M in a constant time slice of AdS_{D+1} . Note that $[M]$ is a set of M polychromatic boundary subregions.

Some of these subregions are anchored with the boundary and rest of the subregions are enclosed within the bulk. Any boundary anchored RT surface encloses a collection of these partitioned bulk subregions. These RT surfaces are therefore homologous to corresponding boundary subregions.

We can construct a partial cube from the RT arrangement⁵. From the geometry-graph duality proved in [5], given a partial cube with a proper choice of boundary vertices and edge weights, one can construct a constant time slice of a holographic geometry for some dimension. The boundary anchored subregions are called *boundary vertices* and all other subregions in the bulk are called *bulk vertices*, see figure 1.

The relation between bitstrings and holographic geometries is manifested by bypassing the graph representations. For a valid HEI (2.2), we consider a contraction map $f : \{0, 1\}^M \rightarrow \text{Im}(f) \subseteq \{0, 1\}^N$ satisfying the homology conditions on the boundary. Here, M and N are determined by the number of terms in the HEI. As we saw above, the sets $\{0, 1\}^M$ and the image $\text{Im}(f) \subseteq \{0, 1\}^N$ of the contraction map are related by the consistent homology conditions, e.g., $y_{A_k} = f(x_{A_k})$ for $\forall k \in [n + 1]$.

The transition from the bitstring picture to the graph picture can be done by the bitstrings satisfying the *isometric condition* with respect to J -dimensional hypercubes $H_{[J]} = (V_{[J]}, E_{[J]})$, i.e.,

$$d_H(x, x') = d_G(\iota_J(x), \iota_J(x')), \quad \forall x, x' \in \{0, 1\}^J, \quad J = M, N \in \mathbb{Z}, \quad (2.9)$$

where $\iota_J : \{0, 1\}^J \rightarrow V_{[J]}$ is a path isometry from the set of J -dimensional bitstrings to the vertex set of the J -dimensional hypercube. For simplicity, we denote the isometric condition by

$$d_H = d_G. \quad (2.10)$$

Even if a graph induced from a set of bitstrings does not satisfy the isometric condition, it could still respect the *adjacency condition*, which is weaker than the isometric condition i.e., if, for $x, x' \in \{0, 1\}^J$,

$$d_H(x, x') = 1, \quad \text{then } d_G(\iota_J(x), \iota_J(x')) = 1. \quad (2.11)$$

Similarly, we write the adjacency condition as

$$d_H \stackrel{\text{adj}}{=} d_G. \quad (2.12)$$

When a map is a non-contraction map, we will see in section 4 that there exists a subgraph induced from a connected subset⁶ of bitstrings that does not satisfy the adjacency condition.

With the isometric condition $d_H = d_G$ with respect to the J -dimensional hypercubes $H_{[J]} = (V_{[J]}, E_{[J]})$ applying to $\{0, 1\}^J$ for $J = M, N$, we have

⁵The proof can be done by repeating the similar proof for theorem 7.17 in [25].

⁶A pair of length J bitstrings, $x, x' \in \{0, 1\}^J$, is said to be *connected* if $d_H(x, x') = 1$. A set of bitstrings x_0, \dots, x_{n-1} forms a *Hamming path* if $d_H(x_i, x_{i+1}) = 1$ for $\forall i = 0, \dots, n - 1$. A *connected subset* $X_{[J]} \in \{0, 1\}^J$ of bitstrings is a subset of $\{0, 1\}^J$ such that there is a Hamming path between any pair of elements in $X_{[J]}$.

1. path isometries, $\iota_M : \{0, 1\}^M \rightarrow V_M$, $\iota_N : \{0, 1\}^N \rightarrow V_N$
2. a graph map associated with a map $f : \{0, 1\}^M \rightarrow \{0, 1\}^N$,

$$\Phi_f : H_M \rightarrow \Phi_f(H_M) \subseteq H_N. \quad (2.13)$$

It should be noted that, first, all the graphs constructed above are unit-weighted graphs. Second, the image graph $\Phi_f(H_M)$ depends on the contraction map f while the domain of the graph map, which is H_M , is the same for any choice of contraction map for the HEI.

We now see that theorem 2.1 is equivalent to the following statement.

- *Any holographic geometry with RT arrangements induced by the map satisfies the HEI.*

Before we clarify the statement, we introduce the *preimage* of an image graph under a graph map and the *kernel* of the graph map.

Definition 2.3 (Preimage of graph map). *Let $\Phi : G_1 \rightarrow G_2$ be a graph map between graphs $G_1 = (V_1, E_1)$ and $G_2 = (V_2, E_2)$. The preimage*

$$PreIm(\Phi(G_1)) := \left(PreIm_V(\phi^V(V_1)), PreIm_E(\phi^E(E_1)) \right) \quad (2.14)$$

of $\Phi(G_1) \subseteq G_2$ under a graph map $\Phi := (\phi^V, \phi^E)$ is

$$\begin{aligned} PreIm_V(\phi^V(V_1)) &:= \{v \in V_1 \mid \phi^V(v) \in V_2\} \\ PreIm_E(\phi^E(E_1)) &:= \{e \in E_1 \mid \phi^E(e) \in E_2\}. \end{aligned} \quad (2.15)$$

Note that the preimage $PreIm_E(\phi^E(E_1))$ contains the edges $e \in E_1$ mapped to self-loops.

The kernel of a graph map is the preimage of a null subgraph⁷.

Definition 2.4 (Kernel of graph map). *The kernel of a vertex map and an edge map of a graph map $\Phi := (\phi^V, \phi^E)$ on a graph $G := (V, E)$ is defined as*

$$\begin{aligned} Ker(\phi^V) &:= \{v \in V \mid \phi^V(v) = \emptyset_V\} \\ Ker(\phi^E) &:= \{e \in E \mid \phi^E(e) = \emptyset_E\} \end{aligned} \quad (2.16)$$

where \emptyset_V and \emptyset_E are the null vertex and the null edge, respectively. We denote by $Ker(\Phi) := (Ker(\phi^V), Ker(\phi^E))$ the kernel of the graph map Φ .

For convenience, we write the set difference of the preimage and the kernel as

$$\mathcal{P}(\Phi(G)) := PreIm(\Phi(G)) \setminus Ker(\Phi). \quad (2.17)$$

We will refer to it as a nontrivial preimage of $\Phi(G)$.

The map Φ_f in (2.13) determines the image graph $\Phi_f(H_M)$ and the preimage $\mathcal{P}(\Phi_f(H_M))$. Any connected subgraph $G_N \subseteq \Phi_f(H_M)$ with a choice of edge weights gives the RHS of

⁷A graph is a null graph if its vertex set and edge set are empty[26].

the inequality. If the contraction map proves the inequality, then, any subgraph $G_M = (V_{G_M}, E_{G_M})$ of H_M that can be mapped to $G_N = \Phi_f(G_M)$ should satisfy the inequality from theorem 2.1. That is, from the induced graphs G_M and G_N with a choice of edge weights for each graph, we can write the discrete entropy inequalities⁸ corresponding to the given HEI, i.e.,

$$\sum_{u=1}^M S_{L_u} \geq \sum_{v=1}^N S_{R_v} \rightarrow \sum_{u=1}^M S_{L_u}^* \geq \sum_{v=1}^N S_{R_v}^*. \quad (2.18)$$

From (2.7), we have

$$\begin{aligned} & \sum_{u=1}^M S_{L_u}^* - \sum_{v=1}^N S_{R_v}^* \\ &= \sum_{(\iota_M(x), \iota_M(x')) \in E_{G_M}} \left(d_H(x, x') - d_H(f(x), f(x')) \right) |(\iota_M(x), \iota_M(x'))| \geq 0 \end{aligned} \quad (2.19)$$

for any choice of edge weights. Here, $S_{R_v}^*$ are the discrete entropies whose edge weights are not optimized after the cut-and-gluing procedure applied to the RT arrangement of the LHS. In general, we have the inequality

$$\sum_{v=1}^N S_{R_v}^* \geq \sum_{v=1}^N S_{R_v} \quad (2.20)$$

Therefore,

$$\sum_{u=1}^M S_{L_u} - \sum_{v=1}^N S_{R_v} = \sum_{u=1}^M S_{L_u}^* - \sum_{v=1}^N S_{R_v}^* \geq 0. \quad (2.21)$$

These subgraphs G_M of H_M are determined by the preimage of G_R under Φ_f , i.e.,

$$\mathcal{P}(\Phi_f(H_M)) = H_M \setminus \text{Ker}(\Phi_f). \quad (2.22)$$

From the geometry-graph duality, a subgraph G_M with a proper set of boundary vertices induces holographic geometries with RT arrangements. All possible ones induced by a subgraph G_M with a proper set of boundary vertices give the LHS of the inequality and satisfy the inequality.

If a map $f : \{0, 1\}^M \rightarrow \{0, 1\}^N$ is a contraction map, all possible holographic geometries giving the LHS are faithfully represented by H_M . That is, $\mathcal{P}(\Phi_f(H_M))$ is a M -dimensional hypercube because the kernel is trivial, i.e., $\text{Ker}(\Phi_f) = (\emptyset_V, \emptyset_E)$. Moreover, any connected subgraphs of $\mathcal{P}(\Phi_f(H_M)) \subseteq H_M$ satisfy the adjacency condition $d_H \stackrel{\text{adj}}{=} d_G$ for the same reason.

3 Lessons from Simple Scenarios

In this section, we will discuss three examples to motivate our proof method and illustrate the underlying physics. This will also help us bridge the physical considerations to mathematical statements.

⁸For the definition of discrete entropy, see definition 2 in [5].

In particular, when one has a non-contraction map, the image graph is i) not a partial cube, ii) a cubical graph, but not a partial cube, and iii) a partial cube. It should be noticed that the image graph being a partial cube is necessary, but not sufficient, for a map to be contractive. The key is that the preimage of the image graph under the graph non-contraction map contains a subgraph that violates the adjacency condition $d_H \stackrel{\text{adj}}{=} d_G$ (2.11). As we will see in section 4, the existence of such a subgraph leads the non-contraction map to induce geometries that do not satisfy a given inequality.

In the first and second examples, we present a geometry induced by the non-contraction maps associated with some given false HEIs. The third example deals with the monogamy of mutual information(MMI) with a non-contraction map. We will see that such a map also induces a geometry that does not satisfy the MMI.

3.1 Deforming the Monogamy of Mutual Information

Consider the MMI inequality

$$S(AB) + S(AC) + S(BC) \geq S(A) + S(B) + S(C) + S(ABC), \quad (3.1)$$

for three disjoint regions A, B, C (and a purifier O), being probed on a static time-slice of AdS_3/CFT_2 , such that the associated bulk entanglement wedges $W(AB), W(AC), W(BC)$ and $W(ABC)$ are connected. The contraction map proof method can be thought of as cutting and gluing RT surfaces. Recall the contraction map proof method from section 2, see figure 2 for a visual demonstration of the same. The RT surfaces associated with regions AB, BC , and CA are drawn in red, blue, and green, respectively (fig 2a). One can cut the red and blue surfaces and glue them such that they are now homologous to regions A and C (shown in purple and orange dashed curves, respectively) (fig 2b), before smoothly deforming them into minimal surfaces homologous to A and C (shown in purple and orange solid curves, respectively). For this particular choice of geometry, the RT surfaces corresponding to AC (drawn in green) is cut and glued as the RT surfaces homologous to B and ABC (fig 2c).

Let us now deform the MMI inequality to,

$$S(AB) + S(AC) + S(BC) \geq S(A) + S(B) + S(C) + S(ABC) + S(AB). \quad (3.2)$$

Clearly, this is a false inequality. We will now discuss what goes wrong at the level of contraction map (see table 1). We append a column to the MMI contraction map corresponding to extra term. We see that after imposing the boundary conditions, we reach a point of conundrum where any bit choice would result in a contradiction, i.e, those bits are simultaneously required to be 0 and 1. What we see here is a false inequality leading to a non-contractive mapping. This feature was observed in a previous work [21].

Using the triality proposed in [15], we will now discuss what it means in the graph picture. We will choose the remaining bits (which gives a non-contraction map) and draw the graph (see figure 3). We see that the image graph has an isometric embedding in H_5 respecting the boundary conditions and is a partial cube. So the image graph being a partial cube is not a sufficient condition, but rather a necessary one for the validity of a

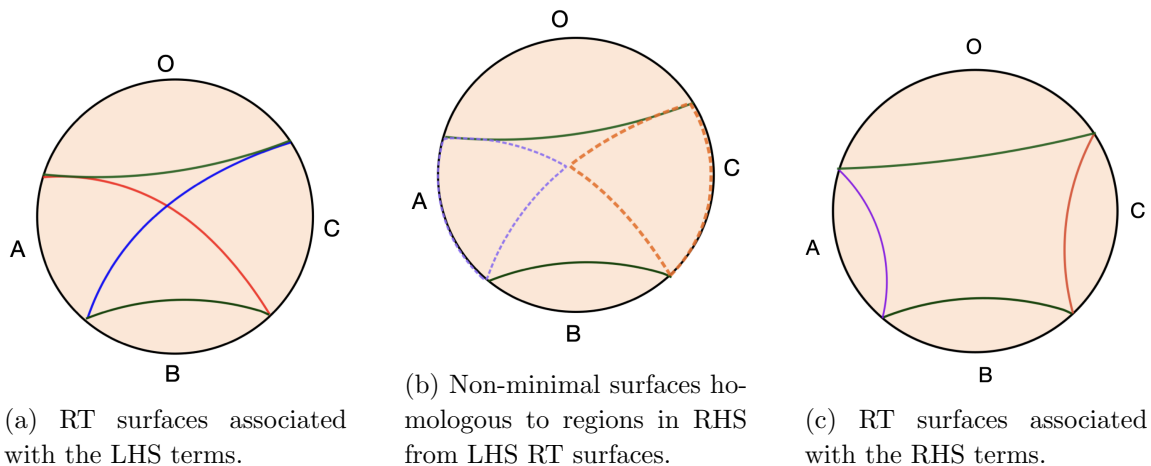


Figure 2: The RT surfaces associated with the LHS terms (2a) is cut and glued (rearranged) to correspond to (non-minimal) surfaces associated with RHS terms (2b) and finally smoothly deformed to their respective minimal surfaces (2c).

	AB	AC	BC	A	B	C	ABC	AB
O	0	0	0	0	0	0	0	0
	0	0	1	0	0	0	1	
	0	1	0	0	0	0	1	
C	0	1	1	0	0	1	1	0
	1	0	0	0	0	0	1	
B	1	0	1	0	1	0	1	1
A	1	1	0	1	0	0	1	1
	1	1	1	0	0	0	1	

Table 1: Failure to fill up the contraction map of inequality 3.2. The empty bits are simultaneously required to be 0 and 1 to satisfy the contraction map condition.

HEI. Looking at the table 1, it is clear that the domain of the graph maps to the image without preserving all adjacent edges. Such a mapping does not take a RT arrangement of graphs to another smoothly. Strictly from a graph picture, this can be traced back to deletion of edges in the original hypercube such that the pre-image is a cubical graph instead of a hypercube. By deleting edges, one violates the adjacency condition $d_H \stackrel{\text{adj}}{=} d_G$ in (2.11) between vertices whose bitstring labels differ by a single bit. Recall that the vertices of the graph in the holographic geometry correspond to bulk subregions, chambered by the RT surfaces. Each such bulk subregion is mapped with a bitstring and two subregions separated by a RT surface differ by a single bit (unless there are zero-volume chambers sitting on the RT surfaces, which are referred as *unphysical bitstrings*). The contraction map can be thought of as an operation on the RT surfaces to be smoothly deformed from one configuration to another. In this example, there is no such continuous deformation of the RT surfaces corresponding to the LHS into those corresponding to the RHS. So, how

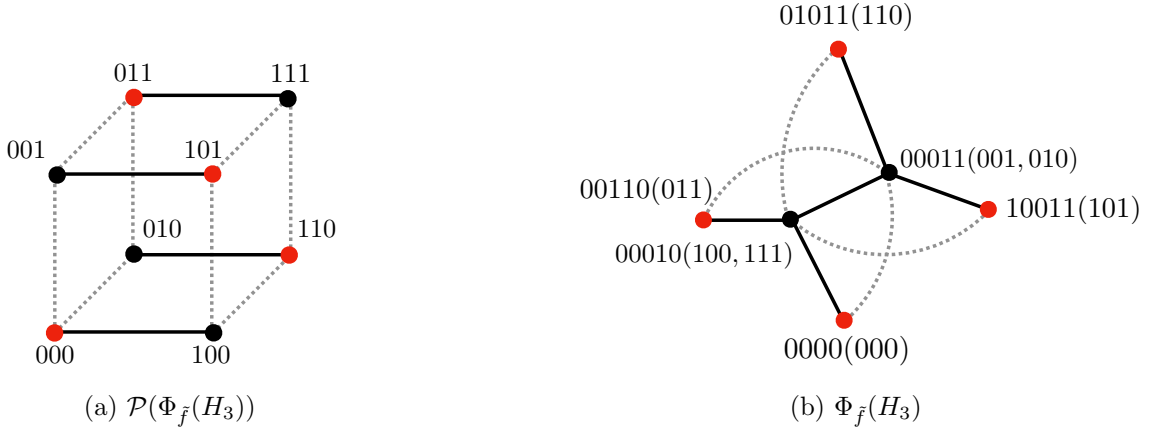


Figure 3: The violations of $d_H \stackrel{\text{adj}}{=} d_G$: The dotted lines emphasize the null edges that violate the adjacency condition. The red circles are the boundary vertices. The black dots are the bulk vertices. (a) The nontrivial preimage $\mathcal{P}(\Phi_{\tilde{f}}(H_3))$ has eight edges missing. Those eight edges belong to the kernel $\text{Ker}(\Phi_{\tilde{f}})$. (b) The image graph $\Phi_{\tilde{f}}(H_3)$ corresponding to the non-contraction map \tilde{f} after choosing the empty bits in the last column to be 1, 1, 0, 0 for the second, third, fifth, and eighth row, respectively.

exactly does this graph mapping differ from those of graph contraction maps [15] (also known as *weak graph homomorphisms*[5])?

In the usual story of graph contraction maps [15], we have a set of hypercube vertices and one identifies some subset of vertices as the same, or equivalently this can be thought of as taking a specific partition of the set of vertices. The new edge after vertex identification are derived from the ones existing before identification, i.e., if two vertices are identified then the set of neighboring vertices is the union of their neighboring vertices before the identification. This ensures that the image graph is always a contraction. However, it is not guaranteed that the image graph is isometrically embeddable in a hypercube. In the case when the image graph can be isometrically embedded in a hypercube, we get a partial cube and a valid HEI. Therefore, we can extract at least two independent conditions for the existence of a HEI, the first is that the image graph is a partial cube, and the second is that the edge map respects the adjacency condition $d_H \stackrel{\text{adj}}{=} d_G$.

In the case of inequality 3.2, while the image graph is a partial cube, there is no partition of vertex sets preserving edge adjacency that can realize the image graph in figure 3. In other words, the associated image graph does not come from a contraction of the hypercube H_3 but rather it comes from a contraction of a cubical graph⁹ (which is a subgraph of H_3). Such cubical graphs, that are not hypercube embeddable, do not correspond to sensible holographic geometries. More precisely, the non-contractiveness and the breakdown of adjacency manifests as a breakdown of the geodesic structure in the bulk.

Therefore we see that a holographic entropy inequality corresponds to a graph mapping from a hyperplane arrangement of a graph to that of another respecting certain adjacency conditions ensuring the existence of a smooth geometry corresponding to the graph. We

⁹Cubical graphs are not always isometrically embeddable in a hypercube.

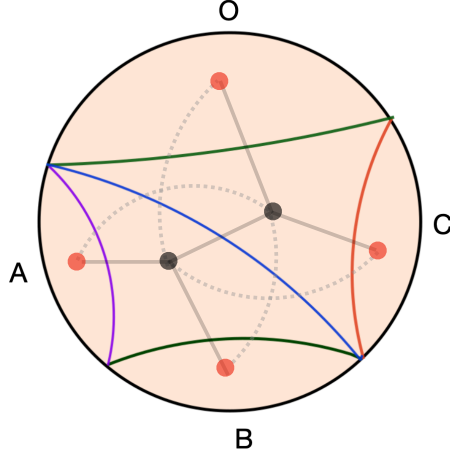


Figure 4: The minimal surface arrangement corresponding to the RHS of inequality 3.2. It is impossible to smoothly deform the configuration of RT surfaces in figure 2a into this configuration by cutting and gluing. It requires the RT surface associated with AB to be deformed and not deformed simultaneously.

will use this insight to prove the completeness of the contraction map proof method.

Before moving on from this example, let us discuss the image graph in terms of the corresponding geometry we chose earlier. It is clear that one can never get the RT surface arrangement of figure 4 by cutting and gluing RT surfaces in figure 2a.

3.2 A Five-Party Example

The inequality considered in subsection 3.1 is neither balanced, nor superbalanced. The example may appear a bit artificial and trivial to the reader. Now we will consider a five-party example,

$$S(BC) + S(ACD) + S(ACE) + S(BCDE) \geq S(AC) + S(BCD) + S(BCE) + S(ACDE), \quad (3.3)$$

which can be rephrased as,

$$I(D : E|AC) - I(D : E|BC) \geq 0 \quad (3.4)$$

where we have defined

$$\begin{aligned} I(X : Y) &:= S(X) + S(Y) - S(XY), \\ S(X|Y) &:= S(XY) - S(Y). \end{aligned} \quad (3.5)$$

Since the inequality 3.3 can be expressed as a difference of mutual information between D and E conditioned on AC and BC respectively, one can choose a geometry where the inequality is violated. Therefore, this is not a valid HEI. As expected, one cannot find a contraction map for this inequality. Using the deterministic rules for filling up the contraction map [21], one reaches a contradiction where a single bit is simultaneously required to be 0 and 1. We plot the graph in figure 5 associated with the partially filled

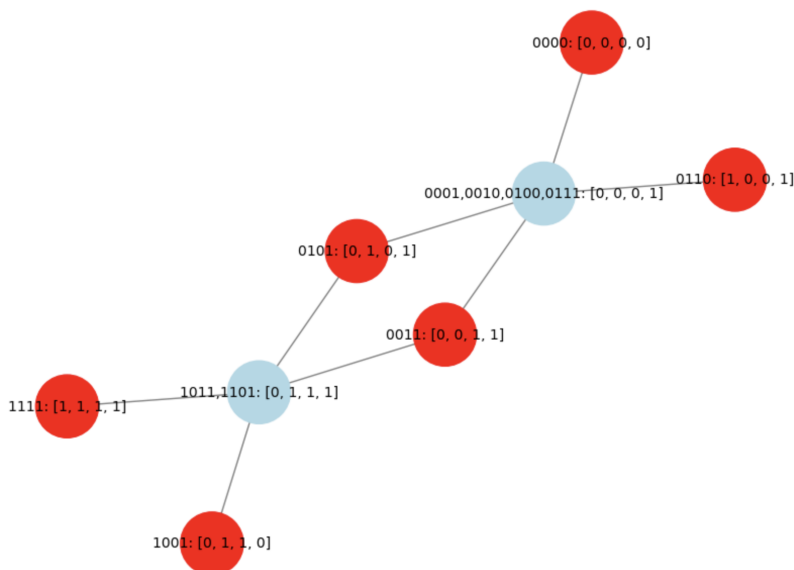


Figure 5: The graph corresponding to the contraction map after choosing the empty bits to be 1, 1, 0, 0 respectively. This graph (encoding the HEI through occurrence bitstrings) does not have an isometric embedding in H_5 . The vertices in red correspond to occurrence bitstrings, and those in light-blue are fixed by the deterministic rules described in [21].

contraction map and see that the image graph is not isometrically embeddable in H_4 ¹⁰. Therefore, the associated inequality is invalid. It is easy to see that this graph is a partial cube and can be embedded in a higher dimensional hypercube (e.g., in H_6). However, this will still yield a false inequality as the graph mapping does not preserve adjacency, i.e., it will yield a mapping where the pre-image does not satisfy the adjacency condition $d_H^{\text{adj}} = d_G$.

3.3 Non-contraction and Geometry

We will now look at an example of how a non-contraction map induces a geometry that does not satisfy the HEIs.

The choice of the boundary conditions we have in table 2 gives the MMI (3.1), but the map \tilde{f} is non-contractive. For example, the bitstring 001 of the second row of table 2 is non-contractive with respect to 000 and 011, i.e.,

$$d_H(001, 000) = 1 < d_H(\tilde{f}(001), \tilde{f}(000)) = 2, \quad (3.6)$$

and

$$d_H(001, 011) = 1 < d_H(\tilde{f}(001), \tilde{f}(011)) = 2. \quad (3.7)$$

Before presenting the example, we clarify here that an inequality is false if and only if no contraction map can be found. An inequality read off from a non-contraction map

¹⁰Note that the remaining four bitstrings are partially fixed to be $f(1000) \rightarrow 0 - -0$, $f(1110) \rightarrow 1 - -1$, $f(1010), f(1100) \rightarrow 0 - -1$. No choice for the remaining bits can give a contraction map.

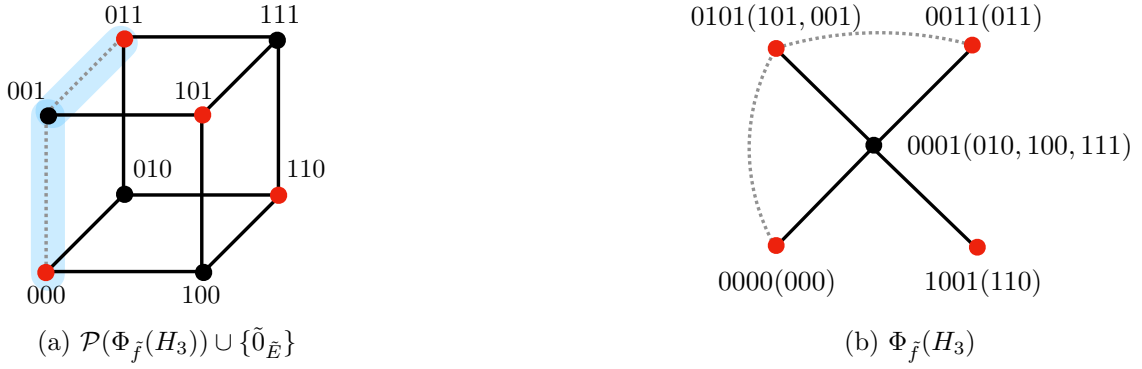


Figure 6: The dotted lines stress the null edges between the vertices that do not satisfy the adjacency condition. (a) The nontrivial preimage $\mathcal{P}(\Phi_{\tilde{f}}(H_3)) \cup \{\tilde{0}_{\tilde{E}}\}$ whose two null edges are replaced by the virtual edges highlighted blue. (b) the image $\Phi_{\tilde{f}}(H_3)$.

does not say anything about its validity. In this section, we provide how a non-contraction map induces a geometry that does not satisfy the MMI. In section 4, we prove that any non-contraction map induces such a geometry. Hence, if one cannot find any contraction map for a given inequality, the inequality is false.

Consider a choice of a connected subset of bitstrings, and its image under the non-contraction map \tilde{f} ,

$$X := \{000, 001, 011, 101, 110, 11\}, \quad \tilde{f}(X) = \{0000, 0001, 0011, 0101, 1001\}. \quad (3.8)$$

With the isometric condition $d_H = d_G$ with respect to the hypercubes H_3 and H_4 , we have the path isometries, ι_M, ι_N , and the graph map $\Phi_{\tilde{f}}$.

Using the path isometries, we have the unit-weighted graphs G and $\Phi_{\tilde{f}}(G) \sim \Phi_{\tilde{f}}(H_3)$ ¹¹, which satisfy the adjacency condition $d_H \stackrel{\text{adj}}{=} d_G$. Then, we can identify the nontrivial preimage $\mathcal{P}(\Phi_{\tilde{f}}(H_3))$ and the image $\Phi_{\tilde{f}}(H_3)$ as in figure 6.

The nontrivial preimage $\mathcal{P}(\Phi_{\tilde{f}}(H_3))$ is a cubical graph where the vertices 000, 001, 011 do not satisfy the adjacency condition $d_H \stackrel{\text{adj}}{=} d_G$. As a result, the edges (001, 011) and (001, 000) are absent. This is simply due to the fact that the kernel $\text{Ker}(\Phi_{\tilde{f}})$ of the graph contraction map $\Phi_{\tilde{f}}$ is non-trivial.

It should be noticed that there is another graph $\tilde{G} = (\tilde{V}_X, \tilde{E}_X)$ whose image graph $\Phi_{\tilde{f}}(\tilde{G})$ under the map $\Phi_{\tilde{f}}$ is also graph isomorphic to $\Phi_{\tilde{f}}(H_3)$. For the map \tilde{f} to give the MMI, any subgraphs of the domain graph that can be mapped to a connected subgraph with a set of proper boundary vertices of the image graph $\Phi_{\tilde{f}}$ should satisfy the inequality as discussed in section 2. Hence, in our case, the subgraphs G and \tilde{G} with the graph non-contraction map should satisfy the inequality for the non-contraction map to give the MMI.

Thus, to verify the inequality, we consider the quantity,

$$\sum_{x, x' \in X} \left(d_H(x, x') - d_H(\tilde{f}(x), \tilde{f}(x')) \right) |(\iota_M(x), \iota_M(x'))|, \quad (3.9)$$

¹¹One can easily check that $\Phi_{\tilde{f}}(G)$ is graph isomorphic to $\Phi_{\tilde{f}}(H_3)$

	AB	AC	BC	A	B	C	ABC
O	0	0	0	0	0	0	0
	0	0	1	0	1	0	1
	0	1	0	0	0	0	1
C	0	1	1	0	0	1	1
	1	0	0	0	0	0	1
B	1	0	1	0	1	0	1
A	1	1	0	1	0	0	1
	1	1	1	0	0	0	1

Table 2: An example of non-contraction map $f : H_3 \rightarrow H_4$ whose boundary conditions give the MMI.

and check its sign. As in (2.19), its sign is positive regardless of the choice of the edge weights if the map \tilde{f} is contractive. When the map \tilde{f} is non-contractive, for instance, $d_H(x, x') + \kappa = d_H(\tilde{f}(x), \tilde{f}(x'))$ for $\kappa \in \mathbb{Z}_+$ and a pair $\tilde{x}, \tilde{x}' \in X$, then, (3.9) is not necessarily positive because of the pair \tilde{x}, \tilde{x}' , i.e.,

$$\sum_{x, x' \in X} \left(d_H(x, x') - d_H(\tilde{f}(x), \tilde{f}(x')) \right) |\iota_M(x), \iota_M(x')| - \kappa \left(d_H(\tilde{x}, \tilde{x}') - d_H(\tilde{f}(\tilde{x}), \tilde{f}(\tilde{x}')) \right) |\iota_M(\tilde{x}), \iota_M(\tilde{x}')|. \quad (3.10)$$

We now see that (3.9) can be negative for \tilde{G} . The key is the edge weights of the edges, such as (001, 000) and (001, 011), which violate the adjacency condition. We call these edges *virtual edges* and are defined in definition 4.3. Without loss of generality, their edge weights can be chosen to be infinite.

Physically, this means that the non-contraction map destroys the smoothness of the bulk geometry. In other words, there are no geodesics between any spatial points in the bulk subregion associated with 001 and any spatial points in that associated with, for instance, 000, see figure 7.

Then, the edge weights of the virtual edges give an infinite value to the second term in (3.10). This results in the sign of (3.10) being negative, and thus violates the MMI.

In the next section, we will see that there is always some holographic geometry where the geodesic structure is altered (and, smoothness of the bulk manifold breaks down) when the corresponding map is a non-contraction map. Thus, for inequality candidates which do not have any contraction map, some holographic geometry will always violate it, and thus, the inequality must be false. Therefore, the existence of a contraction map is necessary for the proof of a valid HEI. We will formalize this statement in the following section 4.



Figure 7: The RT arrangements on $\text{AdS}_3/\text{CFT}_2$ corresponding to the subgraphs G, \tilde{G} : (a) The edge weights of all the edges are associated with the areas of the RT surfaces. (b) The edge weights of the edges colored black are associated with the areas of the corresponding RT surfaces, while the edge weights of the virtual edges highlighted blue are large or infinite. The two blue lines on the constant time slice represent the obstruction to the smoothness of the manifold.

4 Main theorem

Theorem 4.1 (Completeness of contraction map; HEI \leftrightarrow contraction map). *Given a candidate entropy inequality,*

$$\sum_{i=1}^l \alpha_i S_{P_i} \geq \sum_{j=1}^r \beta_j S_{Q_j}, \quad \alpha_i, \beta_j \in \mathbb{Z}_+, \quad (4.1)$$

it is a valid HEI if and only if a contraction map $f : \{0, 1\}^M \rightarrow \{0, 1\}^N$ exists (where $M = \sum_i \alpha_i$ and $N = \sum_j \beta_j$) satisfying homology conditions on the boundary.

From theorem 2.1 [5], the HEI 4.1 is valid if there is a corresponding contraction map. The main contribution of this paper is to prove the converse, i.e., theorem 4.2.

Theorem 4.2 (HEI \rightarrow contraction map). *If the candidate HEI 4.1 is valid, there exists a contraction map.*

Recall that in the holographic dictionary, the RT formula [2] relates the leading order entanglement entropy of a holographic quantum state on the boundary CFT to a minimal surface (RT surface) in the bulk. Therefore, a valid HEI holds for any holographic geometry obeying the RT formula. We take this as the definition of a HEI.

Definition 4.1. *An entropy inequality is a valid HEI if and only if every holographic geometry obeying the RT formula satisfies the inequality.*

Theorem 4.2 is proved by contradiction. We assume, on the contrary, that there exists a valid HEI that does not have any corresponding contraction map. We first prove in lemma 4.2 that, for any non-contraction map, there is at least one geometry that does not

satisfy the inequality. Therefore, from definition 4.1, the inequality cannot be a valid HEI. Hence, theorem 4.2 is proved. Taking theorem 2.1 and theorem 4.2 together, we prove theorem 4.1.

4.1 Mathematical proof

Given a convex combination of entanglement entropies in the inequality (4.1),

$$S_{[l]} := \sum_{i=1}^l \alpha_i S_{P_i}, \quad S_{[r]} := \sum_{j=1}^r \beta_j S_{Q_j}, \quad \alpha_i, \beta_j \in \mathbb{Z}_+, \quad (4.2)$$

or

$$S_M := \sum_{u=1}^M S_{L_u}, \quad S_N := \sum_{v=1}^N S_{R_v} \quad (4.3)$$

for the unimodular sums of (4.2).

We denote the corresponding discrete entropies on a graph by $S_{[l]}^*$, $S_{[r]}^*$ and S_M^* , S_N^* , respectively.

Let us now define a non-contraction map.

Definition 4.2 (Non-contraction map). *A map $\tilde{f} : \{0, 1\}^M \rightarrow \{0, 1\}^N$ is a non-contraction map if, for some $x, x' \in \{0, 1\}^M$,*

$$d_H(x, x') < d_H(\tilde{f}(x), \tilde{f}(x')). \quad (4.4)$$

We assume the following.

Assumption 4.1. *There exists a valid HEI such that there is no corresponding contraction map.*

Based on this assumption, we will check whether there exists a non-contraction map satisfying the homology conditions on the boundary, that satisfies the entropy inequality. For a map to give a HEI, any subgraph of H_M , or equivalently, any RT arrangement on a holographic geometry, induced by the map \tilde{f} satisfies the given HEI. This statement can be unraveled into two folds, similarly discussed in section 2.

First, the choice of a map $\tilde{f} : \{0, 1\}^M \rightarrow \{0, 1\}^N$ fixes the image $Im(\tilde{f}) \subseteq \{0, 1\}^N$. The isometric condition $d_H = d_G$ with respect to the J -dimensional hypercubes $H_{[J]} = (V_{[J]}, E_{[J]})$ for $J = M, N$ in (2.10) induces two objects: i) path isometries, $\iota_M : \{0, 1\}^M \rightarrow V_M$, $\iota_N : \{0, 1\}^N \rightarrow V_N$, and ii) the graph map $\Phi_{\tilde{f}} : H_M \rightarrow H_N$ associated with \tilde{f} . Similarly to the map \tilde{f} , its image graph $\Phi_{\tilde{f}}(H_M) \subseteq H_N$ is fixed by the map \tilde{f} .

Second, if the map \tilde{f} can give an HEI, any subgraph $G_M \subseteq H_M$ with a set of boundary vertices, which can be mapped to a connected subgraph $G_N \subseteq \Phi_{\tilde{f}}(H_M)$, should satisfy the inequality¹². The subgraphs G_M are identified as the subgraphs of the non-trivial preimage $\mathcal{P}(\Phi_{\tilde{f}}(H_M)) \subseteq H_M$ of $\Phi_{\tilde{f}}(H_M) \subseteq H_N$. In this sense, we say that the subgraphs $G_M \subseteq \mathcal{P}(\Phi_{\tilde{f}}(H_M))$, or the corresponding RT arrangements on holographic geometries, are induced by the map \tilde{f} .

¹²This is due to the geometry-graph duality[5].

The strategy of the proof is to show that there exists at least one geometry with an RT arrangement induced by a non-contraction map \tilde{f} that does not satisfy the inequality. This is generally true for any choice of non-contraction maps satisfying the homology conditions on the boundary of the HEI. Hence, it contradicts assumption 4.1. Thus, theorem 4.2 is proved.

Now, we begin the proof. From the isometric condition $d_H = d_G$ with respect to J -dimensional hypercubes $H_{[J]} = (V_{[J]}, E_{[J]})$ for $J = M, N$, we have the path isometries $\iota_M : \{0, 1\}^M \rightarrow V_M$ and $\iota_N : \{0, 1\}^N \rightarrow V_N$ such that

$$\begin{aligned} d_H(x, x') &= d_G(\iota_M(x), \iota_M(x')), \quad \forall x, x' \in \{0, 1\}^M \\ d_H(y, y') &= d_G(\iota_N(y), \iota_N(y')), \quad \forall y, y' \in \{0, 1\}^N. \end{aligned} \quad (4.5)$$

Then, we can construct a graph map from the non-contraction map \tilde{f} with the isometries defined above, i.e., the graph map $\Phi_{\tilde{f}} := (\tilde{\phi}^V, \tilde{\phi}^E)$ consists of a vertex map $\tilde{\phi}^V$ and an edge map $\tilde{\phi}^E$ defined as

$$\tilde{\phi}^V \circ \iota_M := \iota_N \circ \tilde{f}, \quad \tilde{\phi}^E(\cdot, \cdot) := (\tilde{\phi}^V \circ \iota_M(\cdot), \tilde{\phi}^V \circ \iota_M(\cdot)). \quad (4.6)$$

For $x, x' \in \{0, 1\}^M$ satisfying the non-contraction condition (4.4),

$$d_H(x, x') < d_H(\tilde{f}(x), \tilde{f}(x')), \quad (4.7)$$

we have

$$d_G(\iota_M(x), \iota_M(x')) < d_G(\tilde{\phi}^V \circ \iota_M(x), \tilde{\phi}^V \circ \iota_M(x')). \quad (4.8)$$

Now, we state the properties of the graph non-contraction maps.

Lemma 4.1. *For a graph non-contraction map $\Phi_{\tilde{f}} : H_M \rightarrow H_N$, its kernel $Ker(\Phi_{\tilde{f}})$ is non-trivial. Then, $\mathcal{P}(\Phi(H_M))$ is a proper subgraph of the hypercube H_M , i.e., $\mathcal{P}(\Phi(H_M)) \subset H_M$. Equivalently, $\mathcal{P}(\Phi(H_M))$ does not satisfy $d_H \stackrel{adj}{=} d_G$.*

Proof. The kernel of the vertex map is trivial by definition 4.2.

For a non-contraction map $\tilde{f} : \{0, 1\}^M \rightarrow \{0, 1\}^N$ for $M, N \in \mathbb{Z}$. Then, by definition 4.2, there exists an edge $\tilde{e} = (\iota_M(x), \iota_M(x')) \in E_M$ such that

$$d_H(x, x') < d_H(\tilde{f}(x), \tilde{f}(x')). \quad (4.9)$$

As in (4.8), we have

$$d_G(\iota_M(x), \iota_M(x')) = 1 < d_G(\iota_N \circ \tilde{f}(x), \iota_N \circ \tilde{f}(x')) = d_G(\tilde{\phi}^V \circ \iota_M(x), \tilde{\phi}^V \circ \iota_M(x')). \quad (4.10)$$

This implies that the edge $\tilde{\phi}^E(\tilde{e}) = (\tilde{\phi}^V \circ \iota_M(x), \tilde{\phi}^V \circ \iota_M(x'))$ is a null edge, i.e.,

$$\tilde{\phi}^E(\tilde{e}) = \emptyset_E \in E_N. \quad (4.11)$$

Thus, $\tilde{e} \in Ker(\tilde{\phi}^E)$. We denote any edge in $Ker(\tilde{\phi}^E)$ by \tilde{e} from now on.

From definition 2.3 and 2.4, the vertex set \tilde{V}_M and the edge set \tilde{E}_M of $\mathcal{P}(\Phi_{\tilde{f}}(H_M)) = (\tilde{V}_M, \tilde{E}_M)$ are

$$\begin{aligned}\tilde{V}_M &= V_M \setminus \text{Ker}(\tilde{\phi}^V), \\ \tilde{E}_M &= E_M \setminus \text{Ker}(\tilde{\phi}^E).\end{aligned}\tag{4.12}$$

In our case, $\tilde{V}_M = V_M$ because $\text{Ker}(\tilde{\phi}^V) = \{\emptyset_V\}$. With the non-trivial $\text{Ker}(\tilde{\phi}^E)$, we have

$$\mathcal{P}(\Phi_{\tilde{f}}(H_M)) = H_M \setminus \text{Ker}(\Phi_{\tilde{f}}) = (V_M, \tilde{E}_M) \subset H_M.\tag{4.13}$$

It is straightforward to see that $\mathcal{P}(\Phi_{\tilde{f}}(H_M))$ violates the adjacency condition $d_H \stackrel{\text{adj}}{=} d_G$. \square

For later purposes, we will now define *virtual edges*.

Definition 4.3 (Virtual edges). *Consider a graph $G = (V, E)$. We define a virtual edge 0_E between non-adjacent vertices $v, v' \in V$. That is,*

$$0_E := (v, v')\tag{4.14}$$

for $v, v' \in V$ such that

$$d_G(v, v') > 1.\tag{4.15}$$

We set its edge weight $|0_E|$ infinite¹³, i.e.,

$$|0_E| := \infty.\tag{4.16}$$

We can replace the null edges of a graph between non-adjacent vertices with virtual edges without changing the graph structures¹⁴. We assume from now on that the null edge of any graph appearing below is replaced by the virtual edges.

Especially, in our case, there are virtual edges in \tilde{E}_M of $\mathcal{P}(\Phi_{\tilde{f}}(H_M))$ that used to be the edges $\tilde{e} \in \text{Ker}(\tilde{\phi}^E) \subset E_M$ of H_M (see figure 6). We denote those as $\tilde{0}_{\tilde{E}}$. To stress this point, we write the replacement by

$$\tilde{E}_M = E_M \setminus \text{Ker}(\tilde{\phi}^E) \cup \{\tilde{0}_{\tilde{E}}\}.\tag{4.17}$$

Lemma 4.2. *Consider a candidate HEI. For a non-contraction map \tilde{f} satisfying the homology conditions on the boundary of the HEI, there exists at least one geometry that does not satisfy the HEI.*

Proof. By lemma 4.1, we have the graph $\mathcal{P}(\Phi_{\tilde{f}}(H_M))$ for a given non-contraction map. Moreover, the graph has at least one edge $\tilde{0}_{\tilde{E}} = (\iota_M(x), \iota_M(x')) \in \tilde{E}_M$ for $x, x' \in V_M$ such that¹⁵

$$d_H(x, x') = 1 < d_G(\iota_M(x), \iota_M(x')).\tag{4.18}$$

¹³In principle, the edge weight $|0_E|$ can be set to an arbitrarily large but finite value so that it is larger than the maximum distance in G . Without loss of generality, we set it to be infinite.

¹⁴Graph distance between any pairs of vertices is preserved.

¹⁵Note that the graph distance $d_G(\iota_M(x), \iota_M(x'))$ is not infinite since there is a connected path on a connected graph. However, this graph distance is always greater than unit distance.

Let us pick $X \subseteq \{0, 1\}^M$ which has two corresponding graphs $G \subset H_M$ and $\tilde{G} \subset \mathcal{P}(\Phi_{\tilde{f}}(H_M))$. The subgraph \tilde{G} has at least one edge satisfying (4.18). In particular,

$$\begin{aligned} G &= (V_X, E_X) \subseteq H_M \\ \tilde{G} &= (V_X, \tilde{E}_X) \subseteq \mathcal{P}(\Phi_{\tilde{f}}(H_M)) \subset H_M \end{aligned} \quad (4.19)$$

where

$$V_X := \{\iota_M(x) | x \in X\}, \quad E_X := \{(\iota_M(x), \iota_M(x')) | x, x' \in X\}, \quad (4.20)$$

and

$$\tilde{E}_X := E_X \setminus \text{Ker}(\tilde{\phi}^E) \cup \{\tilde{0}_{\tilde{E}}\}. \quad (4.21)$$

The edges $\tilde{e} \in \text{Ker}(\tilde{\phi}^E)$ in G is replaced with $\tilde{0}_{\tilde{E}}$ in \tilde{G} , see figure 6.

To compute the discrete entropy S_i^* for G and \tilde{G} , we elucidate two properties of the graph, such as Winkler classes¹⁶ and the edge weights.

First, the homology conditions and the bitstrings in X determine the Winkler classes $\Theta_u[e]$, or Θ_u , for $u = 1, \dots, M$ of the graphs. This requires that $\tilde{e} = (\iota_M(x), \iota_M(x')) \in \Theta_u$ for G and $\tilde{0}_{\tilde{E}} = (\iota_M(x), \iota_M(x')) \in \Theta_u$ for \tilde{G} .

Second, the weights of the edges (except the virutal edges) in the graphs G and \tilde{G} have been chosen to be unity, so far. Now we will introduce the edge weights associated with the RT arrangement to these graphs. Let us assume that the edges of G and those of \tilde{G} have the same edge weights except \tilde{e} and $\tilde{0}_{\tilde{E}}$. The choice of the edge weights fix the RT arrangement. In particular, the edge weight of the edges in each class Θ_i is fixed by the choice and, thus, so is the area of the RT surface corresponding to the class.

Then, with the choice of edge weights $|e|, |\tilde{e}|$ for $e, \tilde{e} \in E$ for G , the discrete entropy $S_{L_u}^*$ of G is given by

$$S_{L_u}^* = \sum_{e \in \Theta_u} |e| + \sum_{\tilde{e} \in \Theta_u} |\tilde{e}|, \quad (4.23)$$

which is positive semi-definite and can be tuned to be finite. However, the discrete entropy $S_{L_u}^*$ for \tilde{G} is divergent by definition (4.16), i.e.,

$$S_{L_u}^* = \sum_{e \in \Theta_u} |e| + \sum_{\tilde{0}_{\tilde{E}} \in \Theta_u} |\tilde{0}_{\tilde{E}}| = \infty. \quad (4.24)$$

¹⁶

Definition 4.4 (Winkler (equivalence) relation and its equivalence classes[25, 27, 28]). *Consider a connected graph $G = (V, E)$. An edge $e = (v_1, v_2) \in E$ for $v_1, v_2 \in V$ is in Winkler relation Θ to another edge $e' = (v'_1, v'_2) \in E$ for $v'_1, v'_2 \in V$, which is denoted by $e\Theta e'$, if*

$$d_G(v_1, v'_1) + d_G(v_2, v'_2) \neq d_G(v_1, v'_2) + d_G(v_2, v'_1). \quad (4.22)$$

It is an equivalence relation Θ between edges $e, e' \in E$ if the Winkler relation Θ is

1. *reflexive, i.e., $e\Theta e$ for $\forall e \in E$, and*
2. *symmetric, i.e., $e_1\Theta e_2$ implies $e_2\Theta e_1$ for $\forall e_1, e_2 \in E$, and*
3. *transitive, i.e., $e_1\Theta e_2$ and $e_2\Theta e_3$ imply $e_1\Theta e_3$ for $\forall e_1, e_2, e_3 \in E$.*

We denote by $\Theta[e] := \{e' | e\Theta e', \forall e' \in E\}$ the equivalence class of Θ whose representative edge of the class is $e \in E$.

Hence, any geometry realized by \tilde{G} cannot give the proper holographic entanglement entropy.

We now show that the edge weight of $\tilde{0}_{\tilde{E}}$ is the central reason that the inequality cannot hold. For example, consider the edges $\tilde{0}_{\tilde{E}} = (\iota_M(x), \iota_M(x'))$ of \tilde{G} such that

$$d_H(x, x') + \kappa = d_H(\tilde{f}(x), \tilde{f}(x')) \quad (4.25)$$

for some positive integer $\kappa > 0$.

Then, the inequality for $\tilde{G} = (V_X, \tilde{E}_X)$ can be computed by

$$\begin{aligned} S_M^* - S_N^* &= \sum_{(\iota_M(x), \iota_M(x')) \in \tilde{E}_X} \left(d_H(x, x') - d_H(\tilde{f}(x), \tilde{f}(x')) \right) |(\iota_M(x), \iota_M(x'))| \\ &\quad - \kappa \sum_{\tilde{0}_{\tilde{E}} \in \tilde{E}_X} |\tilde{0}_{\tilde{E}}| \geq 0. \end{aligned} \quad (4.26)$$

We used (4.25) to obtain the coefficient κ of the second sum. The first sum is positive semi-definite and finite. However, the second sum is a sum of infinities. Hence, we see that the graph \tilde{G} cannot satisfy the inequality, i.e.,

$$S_M^* - S_N^* = -\infty \geq 0. \quad (4.27)$$

Note that one could have chosen the edge weight of $|\tilde{0}_{\tilde{E}}|$ to be a finite but arbitrarily large value. However, one has a choice to set the edge weight of the virtual edges $\tilde{0}_{\tilde{E}}$ such that the inequality fails.

In short, for any non-contraction map, there is at least one subgraph \tilde{G} in the preimage, which does not satisfy the adjacency condition $d_H \stackrel{\text{adj}}{=} d_G$ and the given holographic (discrete) entropy inequality. This implies that any geometry induced from the subgraph \tilde{G} by the geometry-graph duality cannot satisfy the HEI. Therefore, lemma 4.2 is proved. \square

From lemma 4.2 and definition 4.1, any non-contraction map cannot give the HEI. Hence, theorem 4.2 is proved. Theorem 4.2 and theorem 2.1 prove the completeness of the contraction map, i.e., theorem 4.1.

5 Discussion

5.1 Completeness of the algorithmic method to generate all the HEIs

In [15], we have proposed an algorithm that can generate HEIs by generating all possible partial cubes under graph contraction maps. By construction, it respects the adjacency condition $d_H \stackrel{\text{adj}}{=} d_G$. In that work, we conjectured that this method can generate all the HEIs. In the current work, we prove this result in theorem 4.1. We have not, however, proved the optimality of the algorithm in [15], and further optimizations upon the algorithm are certainly available. Furthermore, we have not completed the full classifications of HEIs, only giving a constructive method for generating them. We will leave the optimization of those methods and this full classification for future work.

Geometrically, it could be interesting to understand what conditions on the geometry must be relaxed in order for non-contracting inequalities to hold. For example, if a GHZ state were desired as the entanglement pattern between multiple CFTs such as that proposed in [29], what manifold conditions would have to be relaxed for this to be permitted?

5.2 Interpretations of the HEIs

It largely remains opaque how to interpret the holographic entanglement entropies heretofore derived; what consequences do they have for holography, or for the subset of quantum states that obey them more broadly? It is known that the cyclic family of inequalities lower bounds the multipartite entanglement of purification and therefore has an operational interpretation [30], but the operational interpretation of the other ones remain opaque. It is possible that they can serve as finer-grained diagnostics for chaos as in [31] in the context of the tripartite information, or as generalizations of the topological entanglement entropy as investigated in [24], but neither approach has yet reached full fruition.

It also remains possible that all holographic entanglement inequalities with either fixed party number or fixed number of LHS terms are derived from an inequality with larger numbers of either quantity, where the entropic contributions of specific subsets of parties have been set to zero. This would certainly be conceptually pleasing, as it would lend at least an alternate mathematical unification of the holographic entanglement entropy inequalities.

5.3 Entanglement wedge nesting and geometry-graph duality

The geometry-graph duality was proposed and proved in [5]. They studied two types of graphs, namely trivalent graphs and partial cubes, in the duality. We utilized partial cubes in this work. They are distinct from the trivalent graphs used in [5, 16, 17, 32–34] in the sense that the vertices of the trivalent graphs are not labeled with the bitstrings of a contraction map. In contrast, the partial cubes are constructed from the contraction maps as discussed in [15]. Since the bitstrings of the contraction maps are expected to follow the inclusion/exclusion principle based on the entanglement wedge nesting (EWN) relations, one would expect the EWN relations in the RT arrangements induced from the partial cubes. However, there are bitstrings that do not seem to satisfy the EWN relations and have been known as *unphysical bitstrings* [21, 35]. Such vertices do not enclose any non-zero volume in the bulk.

Recently, [36] studied and explored the possibility of how the EWN relations constrain the contraction maps. There are three types of EWN violation: The EWN violations i) within a set of bitstrings associated with the LHS of an inequality [21, 35], ii) that of the RHS of the inequality, and iii) between the set of bitstrings of the LHS and that of the RHS. In particular, the authors in [36] mainly considered the effect of the third type in the contraction map method. In our case, the third type is not directly relevant to our proof because the key is whether a map is contractive or non-contractive, or equivalently, whether it satisfies the adjacency condition. In other words, it does not matter how many EWN violations occurred.

However, it would still be interesting to explore the properties of a graph contraction map Φ_f involved with the violations of the third type. This could help us develop an efficient algorithm to find tight HEIs and demystify interpretations of holographic entanglement entropies. We leave further investigations for the future.

Acknowledgments

We would like to thank Sergio Hernandez-Cuenca, Bartłomiej Czech, Hirosi Ooguri, and Michael Walter for helpful comments. N.B. is supported by Northeastern University Department of Physics and by Brookhaven National Laboratory, as well as by the U.S Department of Energy ASCR EXPRESS grant, Novel Quantum Algorithms from Fast Classical Transforms. K.F. and J.N. are supported by Northeastern University.

References

- [1] J. Maldacena, *The Large- N Limit of Superconformal Field Theories and Supergravity.*, *International Journal of Theoretical Physics* **38** (1999) 1113–1133, [[hep-th/9711200](#)].
- [2] S. Ryu and T. Takayanagi, *Holographic derivation of entanglement entropy from the anti-de Sitter space/conformal field theory correspondence*, *Phys. Rev. Lett.* **96** (May, 2006) 181602.
- [3] N. Engelhardt and A. C. Wall, *Quantum Extremal Surfaces: Holographic Entanglement Entropy beyond the Classical Regime*, *JHEP* **01** (2015) 073, [[arXiv:1408.3203](#)].
- [4] C. Akers and G. Penington, *Quantum minimal surfaces from quantum error correction*, *SciPost Phys.* **12** (2022), no. 5 157, [[arXiv:2109.14618](#)].
- [5] N. Bao, S. Nezami, H. Ooguri, B. Stoica, J. Sully, and M. Walter, *The Holographic Entropy Cone*, *JHEP* **09** (2015) 130, [[arXiv:1505.07839](#)].
- [6] T. He, V. E. Hubeny, and M. Rota, *Inner bounding the quantum entropy cone with subadditivity and subsystem coarse grainings*, *Phys. Rev. A* **109** (2024), no. 5 052407, [[arXiv:2312.04074](#)].
- [7] T. He, M. Headrick, and V. E. Hubeny, *Holographic Entropy Relations Repackaged*, *JHEP* **10** (2019) 118, [[arXiv:1905.06985](#)].
- [8] S. Hernández-Cuenca, V. E. Hubeny, and M. Rota, *The holographic entropy cone from marginal independence*, *JHEP* **09** (2022) 190, [[arXiv:2204.00075](#)].
- [9] M. Fadel and S. Hernández-Cuenca, *Symmetrized holographic entropy cone*, *Phys. Rev. D* **105** (2022), no. 8 086008, [[arXiv:2112.03862](#)].
- [10] N. Bao, N. Cheng, S. Hernández-Cuenca, and V. P. Su, *Topological Link Models of Multipartite Entanglement*, *Quantum* **6** (June, 2022) 741.
- [11] B. Czech and S. Shuai, *Holographic Cone of Average Entropies*, *Commun. Phys.* **5** (2022) 244, [[arXiv:2112.00763](#)].
- [12] T. He, S. Hernández-Cuenca, and C. Keeler, *Beyond the Holographic Entropy Cone via Cycle Flows*, *Commun. Math. Phys.* **405** (2024), no. 11 252, [[arXiv:2312.10137](#)].
- [13] R. Bousso and S. Kaya, *Holographic entropy cone beyond AdS/CFT*, *Phys. Rev. D* **111** (2025), no. 8 086014, [[arXiv:2502.03516](#)].

- [14] B. Czech, S. Shuai, and Y. Wang, *Entropy Inequalities Constrain Holographic Erasure Correction*, [arXiv:2502.12246](#).
- [15] N. Bao, K. Furuya, and J. Naskar, *Towards a complete classification of holographic entropy inequalities*, *JHEP* **03** (2025) 117, [[arXiv:2409.17317](#)].
- [16] S. Hernández Cuenca, *Holographic entropy cone for five regions*, *Phys. Rev. D* **100** (2019), no. 2 026004, [[arXiv:1903.09148](#)].
- [17] S. Hernández-Cuenca, V. E. Hubeny, and H. F. Jia, *Holographic entropy inequalities and multipartite entanglement*, *Journal of High Energy Physics* **2024** (2024), no. 8 238.
- [18] B. Czech, S. Shuai, Y. Wang, and D. Zhang, *Holographic entropy inequalities and the topology of entanglement wedge nesting*, *Phys. Rev. D* **109** (May, 2024) L101903, [[arXiv:2309.15145](#)].
- [19] B. Czech, Y. Liu, and B. Yu, *Two infinite families of facets of the holographic entropy cone*, *SciPost Phys.* **17** (2024) 084.
- [20] N. Bao, K. Furuya, and J. Naskar, *A framework for generalizing toric inequalities for holographic entanglement entropy*, *JHEP* **10** (2024) 251, [[arXiv:2408.04741](#)].
- [21] N. Bao and J. Naskar, *Properties of the contraction map for holographic entanglement entropy inequalities*, *JHEP* **06** (2024) 039, [[arXiv:2403.13283](#)].
- [22] N. Bao, K. Furuya, and J. Naskar, *Holographic entanglement entropy inequalities from partial cubes*, [In progress](#).
- [23] N. Bao, C. Cao, M. Walter, and Z. Wang, *Holographic entropy inequalities and gapped phases of matter*, *JHEP* **09** (2015) 203, [[arXiv:1507.05650](#)].
- [24] J. Naskar and S. S. Samal, *Topological entanglement entropy meets holographic entropy inequalities*, [arXiv:2412.05484](#).
- [25] S. Ovchinnikov, *Graphs and Cubes*. Universitext. Springer New York, NY, 2011.
- [26] J. L. Gross and J. Yellen, *Graph theory and its applications*, 2006.
- [27] S. Ovchinnikov, *Partial cubes: structures, characterizations, and constructions*, *Discrete Mathematics* **308** (2008), no. 23 5597–5621.
- [28] P. M. Winkler, *Isometric embedding in products of complete graphs*, *Discrete Applied Mathematics* **7** (1984), no. 2 221–225.
- [29] L. Susskind, *$Er=epr$, ghz , and the consistency of quantum measurements*, 2014.
- [30] N. Bao and I. F. Halpern, *Conditional and multipartite entanglements of purification and holography*, *Physical Review D* **99** (2019), no. 4 046010.
- [31] P. Hosur, X.-L. Qi, D. A. Roberts, and B. Yoshida, *Chaos in quantum channels*, *Journal of High Energy Physics* **2016** (Feb., 2016).
- [32] D. Avis and S. Hernández-Cuenca, *On the foundations and extremal structure of the holographic entropy cone*, *Discrete Applied Mathematics* **328** (2023) 16–39.
- [33] T. He, M. Headrick, and V. E. Hubeny, *Holographic Entropy Relations Repackaged*, *JHEP* **10** (2019) 118, [[arXiv:1905.06985](#)].
- [34] S. Hernández-Cuenca, V. E. Hubeny, and M. Rota, *The holographic entropy cone from marginal independence*, *JHEP* **09** (2022) 190, [[arXiv:2204.00075](#)].

- [35] D. Avis and S. Hernández-Cuenca, *On the foundations and extremal structure of the holographic entropy cone*, *Discrete Appl. Math.* **328** (2023) 16–39, [[arXiv:2102.07535](#)].
- [36] B. Czech and S. Shuai, *Nesting is not Contracting*, [arXiv:2501.17222](#).